Ab initio study on the reaction mechanism of ozone with the chlorine atom

Der-Yan Hwang
Department of Chemistry, Tamkang University, Tamsui 25137, Taiwan

Alexander M. Mebel
Department of Chemistry, Tamkang University, Tamsui 25137, Taiwan and Institute of Atomic and Molecular Sciences, Academia Sinica, P.O. Box 23-166, Taipei 10764, Taiwan

(Received 30 June 1998; accepted 21 September 1998)

Ab initio calculations of the potential energy surface for the $Cl+O_3$ reaction have been performed using the MP2, QCISD(T), CCSD(T), G2, G2M, CASPT2, and MRCI methods with various basis sets. The results show that the reaction pathway can be divided in two parts. The reaction starts on the nonplanar pathway when the Cl atom attacks a terminal oxygen of ozone via TS1, producing a virtual intermediate, a nonplanar chlorine trioxide B. B isomerizes to another virtual intermediate, planar C, which immediately dissociates to $ClO+O_2$ in the coplanar manner. The ClOOO intermediates B and C disappear at the QCISD level of theory. The calculations confirm the direct reaction mechanism for $Cl+O_3$ but the existence of a very flat plateau on the potential energy surface in the region of B, TS2, C, and TS3 can have some effect on the reaction dynamics. TS1 is the critical transition state determining the rate of the $Cl+O_3$ reaction. High level calculations, such as QCISD(T), CCSD(T), MRCI, and CASPT2 with the basis sets from moderate to very large, at the QCISD and CASSCF optimized geometry of TS1, consistently predict the barrier to be about 4–5 kcal/mol, much higher than the experimental value (below 1 kcal/mol). New experimental measurements as well as even higher level theoretical calculations are encouraged in order to resolve this discrepancy. © *1998 American Institute of Physics.* [S0021-9606(98)02948-1]

I. INTRODUCTION

The importance of chlorine species in atmospheric chemistry was first emphasized by Stolarski and Cicerone.[1] The possibility of ozone depletion by chlorine atoms released by the photolysis of chlorofluorocarbons was postulated by Molina and Rowland[2] and supported by several model calculations,[3–5]

$$Cl+O_3 \rightarrow ClO+O_2, \tag{1}$$

$$ClO+O \rightarrow Cl+O_2. \tag{2}$$

The Cl atom plays the role of a catalyst in the ozone depletion reactions (1) and (2). One Cl atom can destroy up to 100 000 O_3 molecules before it is removed by some other reaction. The above mechanism for the destruction of ozone has been supported by the detection of ClO in the stratosphere in recent years.

The reaction $Cl+O_3 \rightarrow ClO+O_2$ is of fundamental importance in stratosphere chemistry.[6–8] Chlorine trioxides have been postulated as a reaction intermediate.[9–15] A direct reaction without intermediate was also proposed from calculations at a semiempirical level.[16]

Although the $Cl+O_3$ reaction has been studied for some 60 years, the details of its mechanism remain obscure.[17] Our object in the present study is to carry out *ab initio* calculations at a sufficiently high level and of sufficient reliability that definitive statements may be made pertaining to the reaction mechanism of ozone with the chlorine atom in strastospheric ozone depletion.

II. COMPUTATIONAL DETAILS

Since the $Cl+O_3$ is known to predominantly give only the ground state $ClO(^2\Pi)+O_2(^3\Sigma_g^-)$ products,[6] we consider here only the ground electronic state potential energy surface. On this surface, full geometry optimizations were run to locate all the stationary points at the HF/6-31G(d), MP2/6-31G(d), MP2/6-311G(d),[18] as well as QCISD/6-311G(d) (Ref. 19) and CASSCF(17,12)/6-311G(d) (Ref. 20) levels of theory. The active space for CASSCF included all valence electrons and orbitals excluding 2s electrons of the oxygen atoms and 3s electrons of Cl. The harmonic vibrational frequencies were obtained at the MP2/6-31G(d), MP2/6-311G(d), and QCISD/6-311G(d) levels in order to characterize the stationary points as minima or first order saddle points, to obtain zero-point vibrational energy corrections (ZPE) and to generate force constant data needed in the IRC calculation. In order to predict more reliable ZPE, the raw calculated ZPE values were scaled by 0.9670 at the MP2/6-31G(d) level and by 0.9748 at the MP2/6-311G(d) level to account for their average overestimation.[21] In several cases, the intrinsic reaction coordinate IRC method[22] was used to track minimum energy paths from transition structures to the corresponding minima. A step size of 0.1 $amu^{-1/2}$ bohr was used in the IRC procedure. The relative energies were initially refined using the G2(MP2) procedure introduced by Pople and co-workers[23] with MP2/6-31G(d) and MP2/6-311G(d) optimized geometries. G2(MP2) theory corresponds effectively to calculations at the QCISD(T)/6-311+G(3df,2p) level with zero-point vibrational energy corrections. For the reactants, $Cl+O_3$, and the critical in-

TABLE I. Total (hartree) and relative (kcal/mol) energies of various compounds in the $Cl+O_3$ reaction, calculated at the MP2 and G2(MP2) levels.

	MP2/6-31G(d)			MP2/6-311G(d)			G2(MP2)[c]// MP2/6-31G(d)		G2(MP2)[d]// MP2/6-311G(d)	
Species	ZPE	E_{tot}[a]	E_{rel}	ZPE	E_{tot}[b]	E_{rel}	E_{tot}	E_{rel}	E_{tot}	E_{rel}
$Cl+O_3$	6.12	684.41255	24.00	6.01	684.55399	20.93	684.77191	37.26	684.77312	37.53
TS1	4.41	684.35574	59.64	4.53	684.49675	56.85	684.76539	41.35	684.76850	40.43
B	7.62	684.40632	27.90	7.47	684.54110	29.01	684.80243	18.10	684.80198	19.42
TS2	7.95	684.40339	29.74	7.83	684.53842	30.70	684.80208	18.33	684.80147	19.74
C	7.98	684.40334	29.77	7.90	684.53835	30.74	684.80220	18.25	684.80156	19.68
TS3	4.73	684.37271	49.00	4.87	684.50990	48.59	684.81881	7.83	684.80702	16.26
$ClO+O_2$	3.23	684.45079	0.00	3.26	684.58734	0.00	684.83128	0.00	684.83293	0.00

[a]The energies include ZPE corrections, calculated at the MP2/6-31G(d) level and scaled by 0.967.
[b]The energies include ZPE corrections, calculated at the MP2/6-311G(d) level and scaled by 0.9748.
[c]The energies are calculated at the MP2/6-31G(d) optimized geometries as $E[\text{QCISD(T)/6-311G}(d)] + E[\text{MP2/6-311+G}(3df)] - E[\text{MP2/6-311G}(d)] + 0.967 \cdot \text{ZPE[MP2/6-31G}(d)]$.
[d]The energies are calculated at the MP2/6-311G(d) optimized geometries as $E[\text{QCISD(T)/6-311G}(d)] + E[\text{MP2/6-311+G}(3df)] - E[\text{MP2/6-311G}(d)] + 0.9748 \cdot \text{ZPE[MP2/6-311G}(d)]$.

coming transition state TS1, additional high level calculations were performed using CCSD(T)/6-311G(d),[24] G2,[25] the G2M(CC), and G2M(CC, MP2) schemes,[26] as well as the multireference MRCI and CASPT2 (Ref. 27) methods with an (11,9) active space and the 6-311G(d), cc-pVTZ, and cc-pVQZ (Ref. 28) basis sets. These calculations were carried out at the QCISD optimized geometry of O_3 and QCISD and CASSCF optimized geometries of TS1. In the multireference calculations, the $Cl+O_3$ reactants were treated as a supermolecule with the Cl atom located 10 Å away from a terminal oxygen of O_3. All the *ab initio* calculations described here were performed employing the GAUSSIAN 94 (Ref. 29) and MOLPRO-96 (Ref. 30) programs.

III. RESULTS AND DISCUSSION

The total and relative energies of various compounds in the reaction of $Cl+O_3$ calculated at the MP2/6-31G(d), MP2/6-311G(d), and G2(MP2) levels of theory are listed in Table I. Table II presents calculated vibrational frequencies. The barriers corresponding to transition state TS1, obtained at various theoretical levels, are collected in Table III. The energy diagram along the reaction path computed at G2(MP2)//MP2/6-311G(d) is shown in Fig. 1. The optimized geometry of various compounds along the predicted pathway of the $Cl+O_3$ reaction are depicted in Fig. 2.

A. Reaction mechanism

At an initial stage, MP2 calculations allowed us to map out roughly the $Cl+O_3$ reaction pathway. As seen in Fig. 2, a nonplanar pathway in the reaction is followed by a planar pathway. The Cl atom attacks ozone in a nonplanar manner and the initial reaction step proceeds via transition state TS1. At MP2/6-31G(d), the Cl–O bond length in TS1 is 2.259 Å indicating of a very early transition state, in accord with the high exothermicity of the process. The ClOO angle is 110.6°, and the ClOOO dihedral angle is 85.2°. This structure is very similar to the nonplanar transition state H—O_3 reported by Dupuis *et al.*[31] The chlorine radical attacks the ozone molecule from the π direction. The MP2/6-31G(d) calculated activation energy is very high, about 36 kcal/mol, but the barrier decreases to 2.9 kcal/mol at G2(MP2)/MP2/6-311G(d). The experimental Arrhenius activation energy for $Cl+O_3$ is 0.34 to about 0.83 kcal/mol.[32,33] We shall discuss the barrier height in the subsequent section. The transition state optimization was followed by the frequency and IRC calculations at the MP2/6-31G(d) level of theory which confirmed that TS1 does connect $Cl+O_3$ and a nonplanar

TABLE II. Vibrational frequencies (cm^{-1}) of various compounds in the $Cl+O_3$ reaction.

Species, method	Frequencies
O_3	
MP2/6-31G(d)	$a_1$727, $a_1$1173, $b_2$2379
MP2/6-311G(d)	$a_1$751, $a_1$1173, $b_2$2281
QCISD/6-311G(d)	$a_1$752, $a_1$1249, $b_2$970
Expt.[a]	$a_1$716, $a_1$1135, $b_2$1089
TS1	
MP2/6-31G(d)	158i, 97, 261, 670, 982, 1077
MP2/6-311G(d)	242i, 120, 303, 693, 948, 1105
QCISD/6-311G(d)	188i, 89, 250, 674, 863, 1017
B	
MP2/6-31G(d)	88, 371, 645, 859, 1165, 2202
MP2/6-311G(d)	86, 373, 662, 872, 1200, 2030
TS2	
MP2/6-31G(d)	30i, 305, 528, 846, 1260, 2618
MP2/6-311G(d)	30i, 308, 533, 836, 1299, 2497
C	
MP2/6-31G(d)	23, 297, 527, 848, 1265, 2623
MP2/6-311G(d)	21, 301, 531, 839, 1304, 2513
TS3	
MP2/6-31G(d)	1061i, 64, 224, 514, 931, 1579
MP2/6-311G(d)	1129i, 71, 229, 534, 917, 1659
ClO	
MP2/6-31G(d)	σ 854
MP2/6-311G(d)	σ 829
O_2	
MP2/6-31G(d)	σ_g1409
MP2/6-311G(d)	σ_g1451

[a]From Ref. 36.

TABLE III. The barrier (in kcal/mol) for the $Cl+O_3 \rightarrow TS1 \rightarrow ClO+O_2$ reaction, calculated at various levels of theory using geometries and ZPE corrections obtained at the QCISD/6-311G(d) level.

Level of theory	$\Delta E^{\#}$	Level of theory	$\Delta E^{\#}$
MP2/6-31G(d)	34.73	G2(MP2)	6.09
MP2/6-311G(d)	36.33	G2M(CC)	4.85
PMP4/6-311G(d)	14.06	G2M(CC,MP2)	6.18
MP2/6-311+G(d)	37.00	CASSCF/6-311G(d)	6.61
PMP4/6-311+G(d)	14.47	CASPT2/6-311G(d)	4.46
MP2/6-311G(2df)	36.26	MRCI/6-311G(d)	6.18
PMP4/6-311G(2df)	12.93	MRCI+D/6-311G(d)	5.81
MP2/6-311+G(3df)	37.81	CASSCF/cc-pVTZ	7.15
QCISD(T)/6-311G(d)	4.61	CASPT2/cc-pVTZ	3.95
CCSD(T)/6-311G(d)	4.70	CASSCF/cc-pVQZ	7.56
G2	4.76	CASPT2/cc-pVQZ	4.33

chlorine trioxide B. The G2(MP2) calculated exothermicity of the $Cl+O_3 \rightarrow B$ reaction step is 18.1 kcal/mol. The structure of B, shown in Fig. 2, is nonplanar and corresponds to a minimum at the UMP2/6-31G(d) and UMP2/6-311G(d) potential energy surfaces. In this structure, the Cl–O bond is fully formed (1.713 Å), with the Cl atom sitting on top of a distorted ozone molecule. The ClOO angle is 107.8°–108.8°, and the ClOOO dihedral angle is 79.3°–81.1°. This structure is very similar to ClOOO optimized at the MP2/6-31G(d) level by Rathmann *et al.*[34]

From the nonplanar B the reaction proceeds to a planar C intermediate via transition state TS2. In the planar structure C, a minimum at the UMP2 potential energy surfaces, the ClO bond is 1.706 Å, with the Cl atom on the same plane with a distorted ozone molecule. At the MP2/6-31G(d) level, the ClO bond length of C is 0.007 Å shorter than that of B and the central O–O bond length of C is 0.006 Å longer than that of B. From B to C, the central O–O bond is weakened, the terminal bond becomes stronger, and the dihedral angle changes from 79.3° to 180°. This finding is in accord with the fact that the next step leading to formation of $ClO+O_2$ involves a cleavage of the central O–O bond. The relative energy of C is 1.84 kcal/mol higher than that of B at the MP2/6-31G(d) level but only 0.26 kcal/mol higher at G2(MP2)//MP2/6-311G(d). Transition state TS2 has a structure very similar to that of C but with the dihedral angle of 164°. The barrier for the $B \rightarrow TS2 \rightarrow C$ transformation is extremely low, 0.32 and 0.06 kcal/mol relative to B and C, respectively, at G2(MP2)//MP2/6-311G(d).

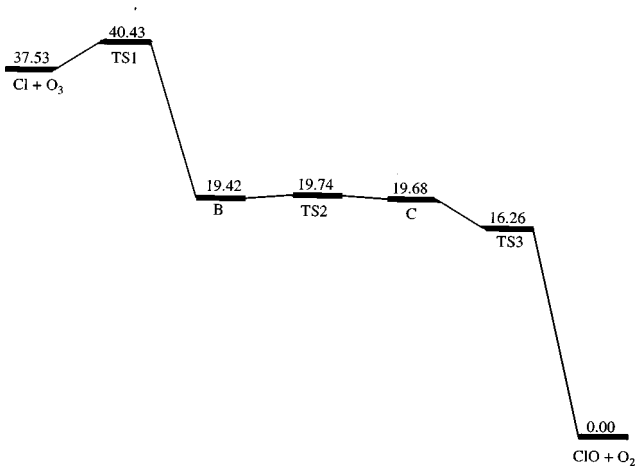

FIG. 1. Potential energy diagram for the $Cl+O_3$ reaction, calculated at the G2(MP2)//MP2/6-311G(d) level.

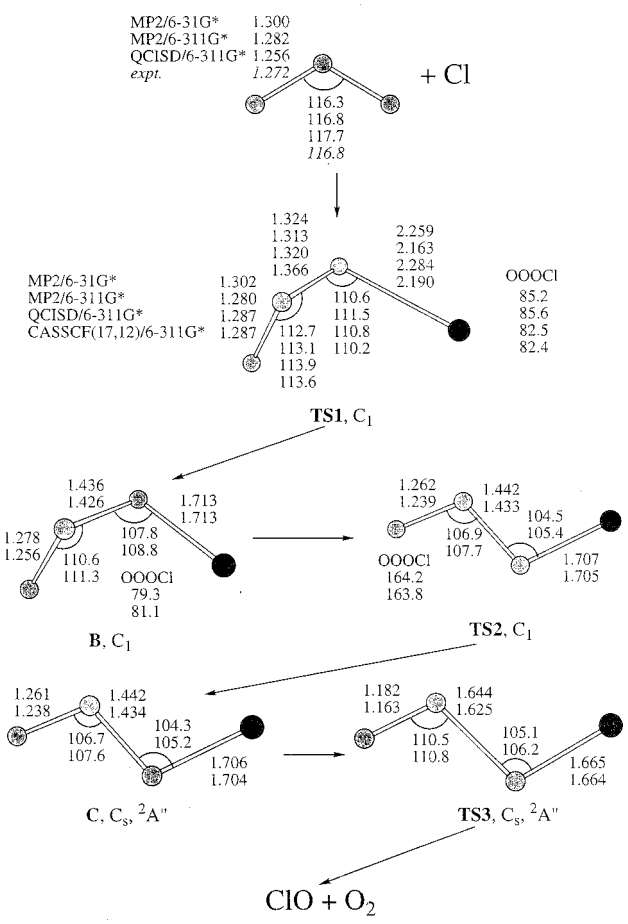

FIG. 2. Optimized geometries of various stationary points along the $Cl+O_3$ reaction pathway, calculated at different levels of theory.

From C, the reaction proceeds by the planar pathway. The transition-state structure for chlorine trioxide $C \rightarrow ClO+O_2$ is TS3. Starting from C, the central O–O bond continues to lengthen, but the dihedral angle keeps 180° all the way. In the transition state TS3, the $ClO-O_2$ distance is 1.644 Å (at MP2/6-31G(d)). Simultaneously, the terminal O–O bond and O–Cl bond become stronger with the bond distances of 1.182 Å and 1.665 Å, respectively. The calculated UMP2/6-31G(d) energies place the transition state 19.23 kcal/mol higher than planar C, and the $ClO+O_2$ at 29.77 kcal/mol below chlorine trioxide C. The UMP2/6-31G(d) IRC calculation confirmed that the first order saddle point TS3 does connect the chlorine trioxide C and $ClO+$triplet-O_2.

The relative stability of C and TS3 changes at higher theoretical levels. The calculated G2(MP2)//MP2/6-311G(d) energies place the transition state TS3 3.4 kcal/mol lower than planar C, and $ClO+O_2$ at 19.7 kcal/mol below C. This implies that the nonplanar B and planar C intermediates may not be stable at this level of theory. In this respect, the result is very similar to the finding by Rauk *et al.*[17] who reported

that the ClOOO minimum disappeared when they used for optimization the restricted open shell RMP2 method. We tried to optimize the geometry of B and C at QCISD/6-311G(d) and a density functional B3LYP/6-311G(d) level,[35] however, the optimization converged to $ClO+O_2$. This indicates that the chlorine trioxide B and C intermediates are unstable at these levels of theory. Therefore, B and C can be called virtual rather than real intermediates.

Geometries of TS1 optimized at the QCISD/6-311G(d) and CASSCF(17,12)/6-311G(d) levels are, in general, similar to those obtained at MP2. At QCISD and CASSCF the central OO bond length is 1.32 and 1.37 Å and ClO distance is 2.28 and 2.19 Å, respectively. As will be discussed below, the higher level energies of TS1 calculated for the QCISD and CASSCF optimized geometries are close despite the notable difference in the ClO distance. The QCISD/6-311G(d) frequencies of the transition state are similar to those computed by the MP2/6-311G(d) method. The deviations of the scaled by 0.9496 (Ref. 21) MP2 frequencies from the QCISD frequencies do not exceed 40 cm^{-1}.

The calculations predict the following reaction pathway: the Cl atom attacks the terminal oxygen in a nonplanar manner through transition state TS1 producing a nonplanar chlorine trioxide B which may or may not be a stable intermediate. Even if B exists, it is a very short-lived species or virtual intermediate which directly dissociates to $ClO+O_2$. The planar chlorine trioxide C could also be passed by because its relative energy is so close to that of B. The present calculations support the conclusion by Zhang and Lee[6] made from their crossed molecular beam study that the $Cl+O_3$ reaction proceeds through a direct reaction mechanism. Meanwhile, the existence of a very flat plateau in the vicinity of B, TS2, C, and TS3 may affect the reaction dynamics. Zhang and Lee raised a possibility of a coplanar reaction pathway in the reaction. We could not find any coplanar transition state for the initial attack of the Cl atom. On the other hand, the dissociation of the virtual intermediates proceeds from the vicinity of C in the coplanar manner which can account for the character of the product scattering observed in experiment.

The calculated heat of this reaction, $\Delta H = -37.5$ kcal/mol at the G2(MP2) level of theory, is in close agreement with the experimental value of -39.1 kcal/mol. We did not include any empirical ''HLC'' corrections[23] in the G2(MP2) energies. Formally, the number of electronic pairs changes from $Cl+O_3$ to $ClO+O_2$. On the other hand, the singlet O_3 molecule has a significant open shell character and the number of electron pairs is not well defined. Also, the formal use of HLC would make $\Delta H = -34.4$ kcal/mol and worsen the agreement with experiment.

B. How high is the reaction barrier?

The activation energy for $Cl+O_3 \rightarrow ClO+O_2$ measured experimentally, 0.34–0.83 kcal/mol,[32] is very low. However, our calculations resulted in a significantly higher value for the reaction barrier. At the G2(MP2)//MP2/6-311G(d) level the calculated barrier at TS1 is 2.9 kcal/mol including ZPE corrections at the MP2 level and the classical barrier is 4.3 kcal/mol. Meanwhile, the MP2/6-311G(d) approximation does not reproduce experimental vibrational frequencies of the ozone molecule; for instance, the b_2 frequency is more than twice overestimated, 2281 cm^{-1} vs 1081 cm^{-1} in experiment.[36] Using the QCISD frequencies we obtain the ZPE of TS1 0.1 kcal/mol lower than the ZPE of the reactants and the G2(MP2) reaction barrier should be corrected to 4.2 kcal/mol, much higher than the experimental activation energy.

In order to confirm this result, we carried out more accurate calculations of TS1. As seen in Table III, the barrier at TS1 computed with the ZPE obtained at the QCISD level using most accurate *ab initio* methods applicable to this system is in the 4–6 kcal/mol range. With the moderate 6-311G(d) basis set, the QCISD(T), CCSD(T), CASPT2, and MRCI+D (MRCI including Davidson's correction) methods resulted in the barrier heights of 4.61, 4.70, 4.46, and 5.81 kcal/mol, respectively. The increase of the basis set gives only insignificant changes; the G2 and G2M(CC) barriers are very close to those obtained by QCISD(T)/6-311G(D) and CCSD(T)/6-311G(d). The use of correlation-consistent Dunning's basis sets does not change the situation; the CASPT2/cc-pVTZ barrier is 3.95 kcal/mol. Using the CASPT2 approach we were able to carry out very extensive calculations with the cc-pVQZ basis set (the total number of contracted basis functions is 224). But the result, 4.33 kcal/mol, is nearly the same as at CASPT2/6-311G(d). Thus, the barrier height is not very sensitive to the basis set extension. Finally, the MRCI and CASPT2/6-311G(d) calculations at the CASSCF/6-311G(d) optimized geometry of TS1 gave the barriers about 0.5 kcal/mol higher than those obtained at the QCISD/6-311G(d) optimized geometry.

Thus, different sophisticated single- and multireference *ab initio* methods consistently predict the $Cl+O_3$ barrier to be in the 4–6 kcal/mol range, much higher than the experimentally measured value. The reason of such a significant deviation is not quite clear. The discrepancy is beyond the accuracy usually expected from the calculational methods used here. Our result appeals for new experimental measurements of the reaction rate constant for $Cl+O_3$. On the other hand, assuming that the experimental activation energy is accurate, the $Cl+O_3$ potential energy surface is a real challenge for even more sophisticated theoretical calculations.

Within the transition state theory (TST), one can calculate the reaction rate constant for $Cl+O_3 \rightarrow TS1 \rightarrow ClO+O_2$. In our computations, we used QCISD vibrational frequencies and moments of inertia of ozone and TS1. The lowest real frequency of TS1 is 89 cm^{-1}, this vibration approximately corresponds to internal rotation around the central OO axis and might be better described as a free or hindered rotor. From the geometry of TS1 we compute the reduced moment of inertia for this rotation to be 32.56×10^{-40} g cm^2. Treating the lowest frequency vibration as a free rotor we obtain the preexponential A factor of 6.66×10^{-11} cm^3 $molecule^{-1}$ s^{-1} at 298 K, twice higher than the experimental value.[32,33] On the other hand, treatment of all the frequencies as harmonic oscillators gives the A factor of 6.93×10^{-12}. The average value of A between the vibrational and free rotor treatment is 3.68×10^{-11} cm^3 $molecule^{-1}$ s^{-1}, close to the

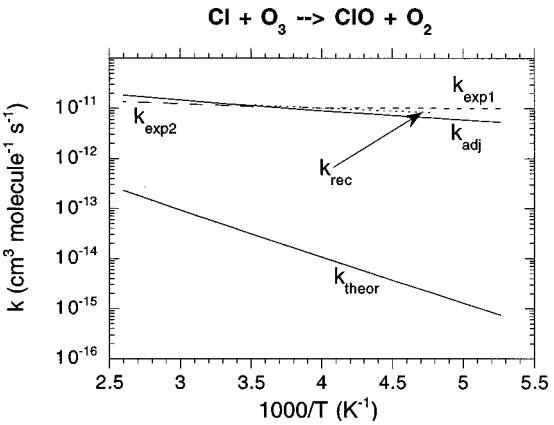

FIG. 3. Arrhenius plots of the calculated and experimental rate constants for the $Cl+O_3 \rightarrow TS1 \rightarrow ClO+O_2$ reaction in the temperature range of 190–385 K. k_{theor}, theoretical rate constant computed with the CASPT2/cc-pVTZ barrier height of 4.0 kcal/mol. k_{adj}, theoretical rate constant computed with the adjusted barrier of 0.65 kcal/mol. k_{exp}, experimental rate constant from Ref. 33, $1.19\times10^{-11}\exp(-33/T)$ $cm^3\,molecule^{-1}\,s^{-1}$ for $189\,K \leqslant T \leqslant 269\,K$. k_{exp2}, experimental rate constant from Ref. 33, $2.49\times10^{-1}\exp(-233/T)$ $cm^3\,molecule^{-1}\,s^{-1}$ for $269\,K \leqslant T \leqslant 385\,K$. k_{rec}, recommended rate constant from Ref. 37, $2.9\times10^{-11}\exp(-260/T)$ $cm^3\,molecule^{-1}\,s^{-1}$ for $205\,K \leqslant T \leqslant 300\,K$.

recommended value of 2.9×10^{-11}.[37] This indicates that a more strict treatment of this vibration as a hindered rotor would be the most accurate.

We use the ''average'' treatment to compute the reaction rates. Figure 3 shows Arrhenius plots of the calculated and experimental rate constants for $Cl+O_3 \rightarrow TS1 \rightarrow ClO+O_2$. Using the theoretical reaction barrier of 4.0 kcal/mol (CASPT2/cc-pVTZ) we obtain the rate constant 280 times lower than in experiment at 298 K. If the reaction barrier is reduced to 0.65 kcal/mol, we are able to reproduce the experimental rate of 1.2×10^{-11} $cm^3\,molecule^{-1}\,s^{-1}$.[37] Fitting the rate constants calculated with the adjusted barrier height in the temperature range of 200–300 K gives the following Arrhenius expression:

$$k_{adj} = 5.37\times10^{-11}\exp(-443.3/T)\,cm^3\,molecule^{-1}\,s^{-1}.$$

As compared with expression recommended from experimental measurements,[37]

$$k_{rec} = 2.9\times10^{-11}\exp(-260/T)\,cm^3\,molecule^{-1}\,s^{-1},$$

k_{adj} has the pre-exponential factor 85% larger and the apparent activation energy 0.36 kcal/mol higher. The fit of k_{theor} computed with the *ab initio* barrier of 4.0 kcal/mol gives the same A factor as for k_{adj} and the activation energy of 4.2 kcal/mol.

IV. CONCLUDING REMARKS

Ab initio calculations of potential energy surface for the $Cl+O_3$ reaction at the G2(MP2)//MP2/6-311G(d) level show that the reaction pathway can be divided in two parts. The reaction starts on the nonplanar pathway when the Cl atom attacks a terminal oxygen of ozone via TS1 producing a very short-lived intermediate, nonplanar chlorine trioxide B. B isomerizes to a planar virtual intermediate C which immediately dissociates to $ClO+O_2$ in the coplanar manner. However, the ClOOO intermediates B and C disappear when optimized at the QCISD/6-311G(d) level. Thus, the calculations confirm the direct reaction mechanism for $Cl+O_3$. The existence of very flat plateau on the potential energy surface in the region of B, TS2, C, and TS3 can affect the reaction dynamics. For instance, the final reaction step is shown to proceed from the vicinity of C along the coplanar pathway which can explain the character of the product scattering found in the crossed molecular beam experiments.[6]

TS1 is the critical transition state determining the reaction rate. Our calculations consistently predict the activation energy to be about 4–5 kcal/mol, much higher than the experimental activation energy (below 1 kcal/mol). Additional experimental measurements as well as even higher level theoretical calculations seem to be necessary in order to resolve this discrepancy.

Among the chemical reactions of ozone depletion in stratosphere, the endothermic steps are photochemical reactions to generate chlorine and bromine free radical. Currently, it is believed that the following reactions are responsible for most of the stratosphere ozone loss:[7,8,38–41]

$$Cl+O_3 \rightarrow ClO+O_2, \quad Br+O_3 \rightarrow BrO+O_2,$$

$$ClO+O \rightarrow Cl+O_2, \quad ClO+ClO \rightarrow Cl_2O_2,$$

$$Cl_2O_2+h\nu \rightarrow Cl+ClO_2, \quad ClO_2 \rightarrow Cl+O_2,$$

$$ClO+BrO \rightarrow Br+Cl+O_2, \quad ClO+BrO \rightarrow Br+OClO.$$

The reaction of ozone with the chlorine atom is exothermic and, if the energy barrier is actually less than 1 kcal/mol, it should be very fast. According to the crossed molecular beam study of Zhang and Lee,[6] the generated ClO radical is vibrationally hot and would readily react with oxygen atoms, $ClO+O \rightarrow Cl+O_2$. The other reactions are either exothermic or have vibrationally hot enough reactants. The energy enriched ClO_2 should be broken to $Cl+O_2$ without additional energy. The ice crystals and volcano ash accelerate the depletion of ozone in the stratosphere. The reason is that the ice crystal and ash can remove the heat of the reactions and shift the equilibrium to the direction of ozone depletion.

ACKNOWLEDGMENTS

We are grateful to Dr. B. C. Wang for useful discussions. Funding from Tamkang University was used to buy the computer equipment used in part of this investigation. A partial support from the Chinese Petroleum Corporation Research Fund and from the National Science Council of the Republic of China is much appreciated. We are thankful to Ms. Y. M. Lee for her help with the search of the Universal Database Access concerning related literature in Chemical Abstracts through the World Wide Web.

[1] R. S. Stolarski and R. J. Cicerone, Can. J. Chem. **52**, 1610 (1974).
[2] M. J. Molina and F. S. Rowland, Nature (London) **249**, 810 (1974).
[3] R. J. Cicerone, R. S. Stolarski, and S. Walters, Science **185**, 1165 (1974).
[4] P. J. Crutzen, Geophys. Res. Lett. **1**, 205 (1974).
[5] S. C. Wofsy, M. B. McElroy, and N. D. Sze, Science **187**, 535 (1975).
[6] J. Zhang and Yuan T. Lee, J. Phys. Chem. A **101**, 6485 (1997).
[7] R. P. Wayne, *Chemistry of the Atmosphere* (Clarendon, Oxford, 1991).
[8] L. T. Molina and M. J. Molina, J. Phys. Chem. **91**, 433 (1987).

[9] A. J. Allmand and J. W. T. Spinks, J. Chem. Soc. **1932**, 599.
[10] G. K. Rollefson and A. C. Byrns, J. Am. Chem. Soc. **56**, 364 (1934).
[11] A. C. Byrns and G. K. Rollefson, J. Am. Chem. Soc. **56**, 2245 (1934).
[12] R. W. Davidson and D. G. Williams, J. Phys. Chem. **77**, 2515 (1973).
[13] W. W. Stuper, R. K. M. Jayanty, R. Simonaitis, and J. Heicklen, J. Photochem. **10**, 163 (1979).
[14] S. S. Prasad and W. M. Adams, J. Photochem. **13**, 243 (1980).
[15] S. S. Prasad, Nature (London) **285**, 152 (1980).
[16] S. C. Farantos and J. N. Murrell, Int. J. Quantum Chem. **14**, 659 (1978).
[17] A. Rauk, E. T. Roux, and Y. Chen, J. Phys. Chem. **97**, 7947 (1993).
[18] W. J. Hehre, L. Radom, P. v. R. Schleyer, and J. A. Pople, *Ab Initio Molecular Orbital Theory* (Wiley, New York, 1986).
[19] J. A. Pople, M. Head-Gordon, and K. Raghavachari, J. Chem. Phys. **87**, 5968 (1987).
[20] (a) H.-J. Werner and P. J. Knowles, J. Chem. Phys. **82**, 5053 (1985); (b) P. J. Knowles and H.-J. Werner, Chem. Phys. Lett. **115**, 259 (1985).
[21] A. P. Scott and L. Radom, J. Phys. Chem. **100**, 16512 (1996).
[22] C. Gonzalez and H. B. Schlegel, J. Phys. Chem. **94**, 5523 (1990).
[23] L. A. Curtiss, K. Raghavachari, and J. A. Pople, J. Chem. Phys. **98**, 1293 (1993).
[24] G. D. Purvis III and R. J. Bartlett, J. Chem. Phys. **76**, 1910 (1982).
[25] L. A. Curtiss, K. Raghavachari, G. W. Trucks, and J. A. Pople, J. Chem. Phys. **94**, 7221 (1991).
[26] A. M. Mebel, K. Morokuma, and M. C. Lin, J. Chem. Phys. **103**, 7414 (1995).
[27] (a) H.-J. Werner and P. J. Knowles, J. Chem. Phys. **89**, 5803 (1988); (b) P. J. Knowles and H.-J. Werner, Chem. Phys. Lett. **145**, 514 (1988); (c) H.-J. Werner, Mol. Phys. **89**, 645 (1996).
[28] T. H. Dunning, Jr., J. Chem. Phys. **90**, 1007 (1989).
[29] GAUSSIAN 94, Revision E.3, M. J. Frisch, G. W. Trucks, H. B. Schlegel, P. M. W. Gill, B. G. Johnson, M. A. Robb, J. R. Cheeseman, T. Keith, G. A. Petersson, J. A. Montgomery, K. Raghavachari, M. A. Al-Laham, V. G. Zakrzewski, J. V. Ortiz, J. B. Foresman, J. Cioslowski, B. B. Stefanov, A. Nanayakkara, M. Challacombe, C. Y. Peng, P. Y. Ayala, W. Chen, M. W. Wong, J. L. Andres, E. S. Replogle, R. Gomperts, R. L. Martin, D. J. Fox, J. S. Binkley, D. J. Defrees, J. Baker, J. P. Stewart, M. Head-Gordon, C. Gonzalez, and J. A. Pople, Gaussian, Inc., Pittsburgh, Pennsylvania; 1995.
[30] MOLPRO is a package of *ab initio* programs written by H.-J. Werner and P. J. Knowles, with contributions from J. Almlöf, R. D. Amos, M. J. O. Deegan, S. T. Elbert, C. Hampel, W. Meyer, K. Peterson, R. Pitzer, A. J. Stone, P. R. Taylor, and R. Lindh.
[31] M. Dupuis, G. Fitzgerald, B. Hammond, W. A. Lester, Jr., and H. F. Schaefer III, J. Chem. Phys. **84**, 2691 (1986).
[32] M. S. Zahniser, F. Kaufman, and J. G. Anderson, Chem. Phys. Lett. **37**, 226 (1976).
[33] J. M. Nicovich, K. D. Kreutter, and P. H. Wine, Int. J. Chem. Kinet. **22**, 399 (1990).
[34] T. Rathmann and R. N. Schindler, Chem. Phys. Lett. **190**, 539 (1992).
[35] (a) A. D. Becke, J. Chem. Phys. **98**, 5648 (1993); (b) C. Lee, W. Yang, and R. G. Parr, Phys. Rev. B **37**, 785 (1988).
[36] (a) A. Barbe, C. Secroun, and P. Jouve, J. Mol. Struct. **49**, 171 (1974); (b) T. Tanaka and Y. Morino, J. Mol. Spectrosc. **33**, 538 (1970).
[37] R. Atkinson, D. L. Baulch, R. A. Cox, R. F. Hampson, Jr., J. A. Kerr, and J. Troe, J. Phys. Chem. Ref. Data **21**, 1125 (1992).
[38] M. B. McElroy, R. J. Salawitch, S. C. Wofsy, and J. A. Logan, Nature (London) **321**, 759 (1986).
[39] J. G. Anderson, D. W. Toohey, and W. H. Brune, Science **251**, 39 (1991).
[40] J. W. Barrett, P. M. Solomon, R. L. de Zafra, M. Jaramillo, L. Emmons, and A. Parrish, Nature (London) **336**, 455 (1988).
[41] S. Solomon, Nature (London) **347**, 347 (1990).